Physics Procedia

Volume 75, 2015, Pages 1050–1057

20th International Conference on Magnetism

Magnetic Anisotropy of Maghemite Nanoparticles Probed by RF Transverse Susceptibility

A. I. Figueroa[1,2], J. Bartolomé[1], L. M. García[1], F. Bartolomé[1], A. Arauzo[3], A. Millán[1], and F. Palacio[1]

[1] Instituto de Ciencia de Materiales de Aragón. CSIC-Universidad de Zaragoza, Departamento de Física de la Materia Condensada, E-50009 Zaragoza, Spain

[2] Magnetic Spectroscopy Group, Diamond Light Source, Didcot, OX11 0DE, UK

[3] Servicio de Medidas Físicas, Universidad de Zaragoza, E-50009 Zaragoza, Spain

Abstract

We present radio frequency magnetic transverse susceptibility measurements on γ-Fe_2O_3 nanoparticles, which yield an estimation of their effective anisotropy constant, K_{eff} as a function of nanoparticle size. The resulting values range from 4 to 8 $\times 10^4$ erg/cm^3, being on the order of the magnetocrystalline anisotropy in bulk maghemite. K_{eff} values increase as the particle diameter increases. Evidences of anisotropy field distribution given by the size distribution in the samples, and interparticle interactions that increase as the particle size increases, are also observed in the TS measurements. The effects of such interparticle interaction overcome those of thermal fluctuations, in contrast with the behavior of other iron oxide particles.

Keywords: Magnetic nanoparticles, magnetic anisotropy, iron oxide, transverse susceptibility

1 Introduction

The understanding of the basic physical properties of magnetic nanoparticles (NPs) is nowadays one of the most active fields in research due to their importance for nanoscience and nanotechnology. Their potential technological applications require a total comprehension and control of their fundamental magnetic properties, including their saturation magnetization and anisotropy constants, which may differ from those of their bulk counterpart. Iron oxide nanoparticles are probably the most commonly and widely studied NPs systems given their relatively easy production by chemical routes, and their promising magnetic properties [1, 2, 3]. In particular, the chemical stability of the maghemite (γ-Fe_2O_3) phase[4] makes this system one of the most attractive materials for technological and biomedical applications.

Bulk maghemite has an inverse-spinel structure with some vacant sites, exhibiting ferrimagnetic ordering below 918 K.[4, 5] Maghemite nanoparticles show reduced saturation magnetization compared to the bulk (finite size effect) since the particle's surface plays an important role at the nanoscale [6]. The magnetism of the γ-Fe_2O_3 particles we study in the present work

 Selection and peer-review under responsibility of the Scientific Programme Committee of ICM 2015

doi:10.1016/j.phpro.2015.12.174

may be understood in the frame of a core-shell model, which we summarize as follows [7, 2]: the particles consist of a core with structural periodicity exhibiting a superparamagnetic behavior, and a disordered shell without the periodicity. Most of the magnetic contribution of the entire particle usually originates from the bulk-like ferrimagnetic core. The disordered shell at the surface is analyzed as paramagnetic or antiferromagnetic component in the magnetization data at high fields. The magnetic interaction between the core and the shell can appear as an exchange bias effect. The shell has a thickness of about 1 nm, independently of the size of the particle [7, 2]. A previous study on the effects of pressure on these maghemite nanoparticles allowed to disentangle the contribution of the core ($K_{\rm core}$) and the surface ($K_{\rm S}$) to the effective magnetic anisotropy of the system, $K_{\rm eff}$ [8]. $K_{\rm core}$ values, on one hand, were found to be between that from the magnetocrystalline anisotropy for bulk maghemite and that usually found in maghemite nanoparticles ($10^5 - 10^6$ erg/cm^3). On the other hand, $K_{\rm S}$ is similar to that previously found for maghemite nanoparticles (10^{-2} erg/cm^2). In this work, we study the magnetic anisotropy of maghemite nanoparticles of different sizes, estimated from the direct measurement of the anisotropy field $H_{\rm K}$ from radio frequency (RF) transverse susceptibility (TS) measurements. This technique has been used over the years with great success to study the anisotropy of different systems of magnetic nanoparticles [9, 10] including iron oxide NPs [11, 12].

2 Material and methods

The series of maghemite nanoparticles samples were dispersed in a polymer matrix with low size dispersion and regular distribution of particles. A total of four γ-Fe_2O_3 NPs samples were studied, with average diameters of 5.2, 6, 7 and 13 nm, labeled S5 to S8 following the nomenclature used in Refs. [7, 2]. The NPs diameter has been determined by transmission electron microscopy (TEM) and small angle x-ray scattering, as described in the same references [7, 2]. The average diameter and width obtained from the size distributions for the four samples are listed in table 1. The volume fraction of maghemite in the samples was estimated from the ratio of iron in the sample, the density of maghemite (4.9 g/cm^3), and the density of the polymer (0.975 g/cm^3). The obtained values were 0.019, 0.037, 0.075 and 0.126 for samples S5 to S8 respectively. Considering the particle size, the corresponding interparticle separations were 7.1, 7.3, 6.4 and 6.3 nm.

TS measurements were performed using a RF self-resonant circuit oscillator based on a simple inverter cell using CMOS transistors in cross-coupled topology. The sample in powder form is placed in a gel-cap that snugly fits into the core of an inductive copper coil (L), which is part of the self-resonant circuit oscillator operating a frequency of around 12 MHz. This is inserted into the sample space of a commercial physical property measurement system (PPMS) from Quantum Design using a customized RF coaxial probe. The temperature, T, and static magnetic field, $H_{\rm DC}$, are varied using the PPMS, between 2-300 K and $\pm$10 KOe, respectively. The oscillating RF field, $H_{\rm RF}$, produced by the RF current flowing in the coil windings, is oriented perpendicular to the static field and this arrangement sets up the transverse geometry. In the experiment, a bipolar TS scan is performed at a fixed temperature, where the shift in the resonant frequency is measured as the static field is varied from positive to negative saturation, and viceversa. The frequency shift, Δf, arises from a change in the coil inductance L, determined by the change in the transverse permeability μ_T of the sample, which is, at the same time, proportional to the transverse susceptibility, χ_T. The quantity of interest is the TS ratio, which is expressed as

Table 1: Summary of the parameters deduced from the TEM and magnetic measurements on γ-Fe_2O_3 NPs. S, sample label. Average particle diameter ($\langle D \rangle$) and width (σ) of the size distribution obtained from TEM, blocking temperature (T_M) obtained from TS, saturation magnetization (M_S), anisotropy field (H_K) and anisotropy constant (K_{eff}), these last three parameters at $T = 5$ K. Uncertainties are ±15%, ±5 K, ±9 emu/cm^3, ±30 Oe and ±12% for $\langle D \rangle$, T_M, M_S, H_K and K_{eff}, respectively.

S	$\langle D \rangle$ (nm)	σ (nm)	T_M (K)	M_S (emu/cm^3)	H_K (Oe)	K_{eff} (10^4 erg/cm^3)
S5	5.2	0.9	25	217	340	3.7
S6	6	1.1	105	237	460	5.4
S7	7	1.4	140	210	570	6.0
S8	13	3.2	250	356	440	7.8

$$\frac{\Delta\chi_T}{\chi_T}\% = \frac{\chi_T^{Sat} - \chi_T(H_{DC})}{\chi_T^{Sat}} \times 100 \propto \frac{\Delta f}{f_0}\% \quad (1)$$

where, χ_T^{Sat} is the transverse susceptibility at the saturating field $H^{Sat} = 10$ kOe. A complete description of the measurement system can be found in Ref. [13].

3 Results and discussion

In Fig. 1(a) we show the 3D plot of unipolar TS scans for particles with $\langle D \rangle = 5.2$ nm. For low temperatures the curves show two peaks with different heights but located symmetrically about the origin of the field axis. According to the theoretical model of TS developed by Aharoni *et al.*, [14] a unipolar scan should reveal the existence of two peaks at the anisotropy fields, H_K, and a third one at the switching field, H_S. The absence of the peak at H_S in the TS scans, as in our case or in of similar NP systems, [9] is attributed to the presence of a distribution in anisotropy fields in the system, which causes the peak at the switching field to merge indistinguishably with one of the peaks at the anisotropy field.

As temperature increases from 2 K, the peak heights difference is reduced, and the double-peak structure is less pronounced, evolving into a single central peak, as depicted in the TS bipolar scans plotted for selected temperatures in Fig. 1(b). This trend is consistent with a gradual transition from a blocked state towards a superparamagnetic one [9, 12]. A better illustration of this evolution is observed in the plot of the H_K values (obtained directly from the TS scans) as a function of T shown in Fig. 1(c). From these plots, the T_M of each sample is directly obtained as that value where H_K =0.

Analogous results for the TS measurements have been obtained for the other three samples. T_M values for the four samples are listed in table 1. They are found to decrease as the NP diameter decreases, from 250 K down to 25 K for particles of 13 nm and 5.2 nm, respectively. This trend in T_M may be understood as due to the decrease of the particles magnetic moment with their reduced volume, and, correspondingly, the decrease of their dipole-dipole interactions, similarly to what was observed for $Fe_{3-x}O_4$ NPs in Ref. [12].

As it has been mentioned above, there is a difference in the peaks height of the TS profiles, so that for each unipolar scan from positive to negative field sweep, the peak at the first quadrant is always larger than the peak height in the second one. This feature is better illustrated in Fig.

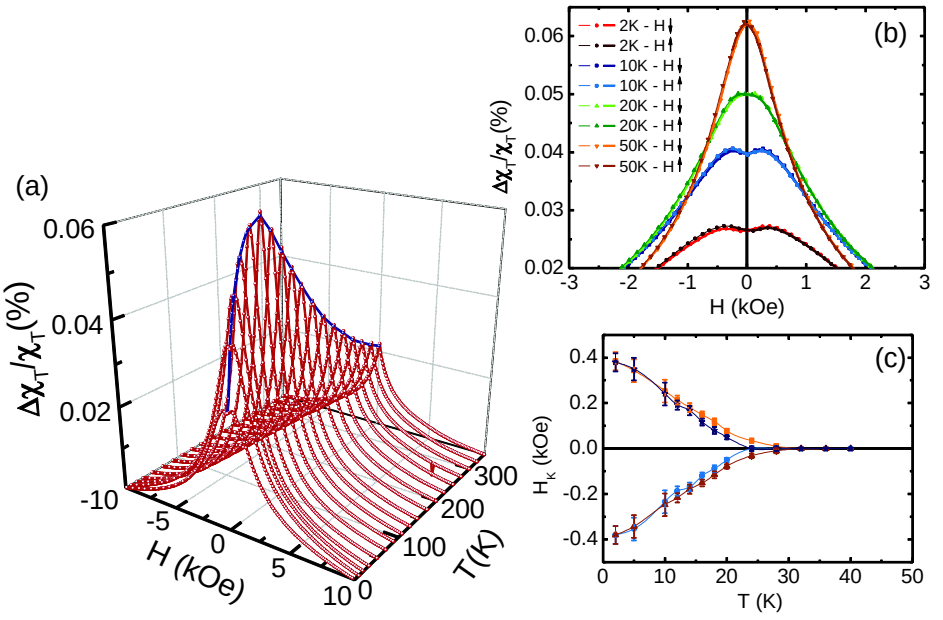

Figure 1: TS results on the sample with $\langle D \rangle = 5.2$ nm. (a) 3D plot of TS unipolar scans at several temperatures. (b) TS bipolar scans at selected temperatures. (c) Values of H_K extracted from the TS scans plotted as a function of T.

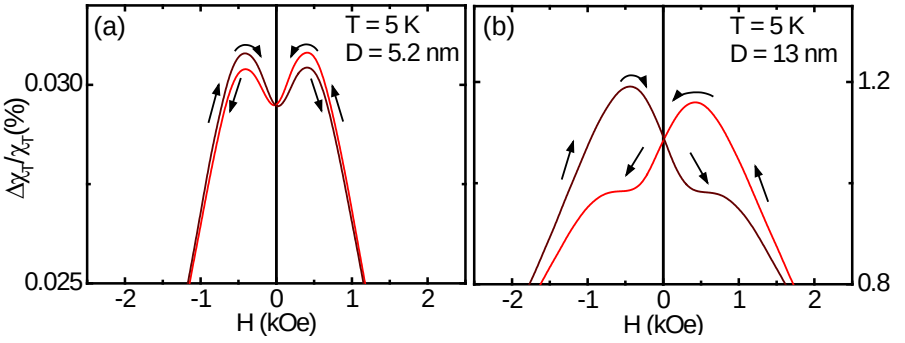

Figure 2: Comparison of the details of the TS bipolar scans measured at $T = 5$ K for the sample with (a) $\langle D \rangle = 5.2$ nm (S5) and that with (b) $\langle D \rangle = 13$ nm (S8). Arrows show the direction of the field sweep.

2 where details of a TS bipolar scan of sample S5 (Fig. 2(a)) and S8 (Fig. 2(b)) measured at $T = 5$ K are shown. One way to analyze such an asymmetry is to quantify the peak difference for each unipolar TS scan as

$$\Delta\text{height}(\%) = \frac{[(\text{Peakheight})_{1^{\text{st}}} - (\text{Peakheight})_{2^{\text{nd}}}]}{(\text{Peakheight})_{1^{\text{st}}}}\%$$

similar to the procedure described in Ref. [9]. In Fig. 3(a) we have plotted Δheight as a function of the reduced temperature T/T_M for the four samples in the series. It is evident that the asymmetry is found to increase as the particle size increases. This is a fact that has been consistently observed in several TS studies of NPs systems and has been related to the presence of anisotropy field dispersion [15], and also as a consequence of increasing interparticle interactions with increasing particle size [9]. Both components might be present in our maghemite NPs samples since, on one hand, previous studies have shown a broader size distribution for the sample with larger diameter than those with smaller ones [2, 7], and, on the other hand, effects of interparticle interactions have been observed in ac susceptibility measurements at different frequencies in these samples. The extrapolated values of the microscopic characteristic time, τ_0, are obtained from a typical Arrhenius plot of $\ln(1/\omega)$ vs. $1/T_B$, where T_B corresponds to the blocking temperature of the particle system, obtained from frequency dependent ac susceptibility measurements. These plots are shown in Fig. 4. For non-interacting superparamagnetic maghemite nanoparticles τ_0 values are usually on the order of 10^{-10} s, while in the present case, τ_0 obtained from linear fits of data shown in Fig. 4 reaches 10^{-15} s for the particles with D = 13 nm. Such a strong reduction in τ_0 is a signature of systems where interparticle interactions are significant [16]. These results reveal an increase in interparticle interactions with NP diameter, which is consistent with the increase of core volume (V_{core}) of the particle, on the one hand, and taking into account that the interparticle separation varies little for these samples (between 6.3 and 7.1 nm, as described above), on the other hand.

The thermal evolution of H_{K} for the four samples is shown in Fig. 3(b). H_{K} are also plotted as a function of the reduced temperature T/T_M in order to have a better comparison. The strong temperature dependence accounts for both the magnetocrystalline anisotropy constant, which we consider negligible in this case, and for the influence of the thermal energy of the particles [17, 18]. The decrease of H_{K} with increasing T is usually described by the equation $H_{\text{K}} = H_{\text{K0}}[1 - (T/T_M)^{\beta}]$, where $\beta \sim 0.5$ [19, 20], for an assembly of aligned particles, and $\beta \sim 0.77$ for an assembly of randomly oriented particles [21, 22, 23], and H_{K0} corresponds to the intrinsic anisotropy field of the material. The emerging picture is that, at low temperatures (e.g. $T = 5$ K), the magnetite particles are frozen and $H_{\text{K}} \sim H_{\text{K0}}$. In fact, H_{K} values at low temperatures are of the same order for all our samples, which suggests that the low-temperature anisotropy field corresponds to the average intrinsic anisotropy field (magnetocrystalline, surface and shape contributions) in all samples.

The curvature of the $H_{\text{K}}(T/T_M)$ plots in Fig. 3(b), is not actually characteristic of a function with $\beta < 1$, as described above, but, instead a curve with $\beta > 1$, characteristic for systems where dipolar interparticle interactions and anisotropy field distribution are relevant [12]. This suggests that the effects of interparticle interactions in this maghemite system overcome those of thermal fluctuations, in contrast with TS results obtained for other iron oxide particles such as SiO_2 - coated $Fe_{3-x}O_4$ NPs described in Ref. [12].

The effective anisotropy constant, K_{eff} may be estimated from the M_{S} obtained from conventional SQUID magnetometry [2] and the values of H_{K} extracted from the TS measurements, as $K_{\text{eff}} = 1/2\ M_{\text{S}}H_{\text{K}}$. The values of H_{K} and M_{S} for each sample, both at $T = 5$ K, used to calculate K_{eff} and the resulting values of the latter are given in table 1 and plotted in Fig. 5. K_{eff}

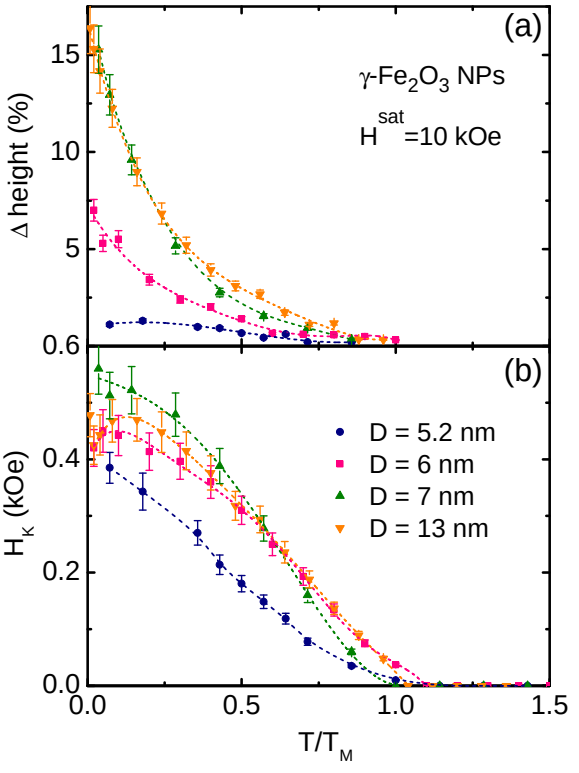

Figure 3: Comparison of (a) the anisotropy peak height difference and (b) $H_{\rm K}$ values extracted from the TS scans, both plotted as a function of T/T_M in the four maghemite NPs samples. Dashed lines are guides to the eye.

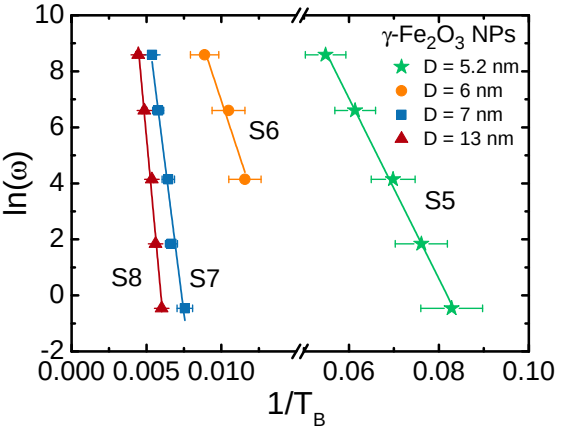

Figure 4: Arrhenius plot of the measuring time $(1/\omega)$ as a function of $1/T_B$, as obtained from ac susceptibility measurements in the four maghemite NPs.

values are on the same order of those reported for the magnetocrystalline anisotropy in bulk maghemite (2.0×10^4 erg/cm^3) [24]. K_{eff} is found to increase as the particle diameter increases, which is consistent with the increase in the anisotropy as the V_{core} in the particles increases, as reported in Ref. [8]. Comparing to those values obtained for the same maghemite NPs in Ref. [8] (being of 7.7×10^5 erg/cm^3 for the core contribution of particles of 6 nm in diameter) our K_{eff} values are found to be lower in almost one order of magnitude. This difference may stem from the influence of the interparticle interactions in the position of H_{K} peaks in the TS scans, as it has been observed in similar NPs systems where the anisotropy field is found to increase with increasing interactions [9].

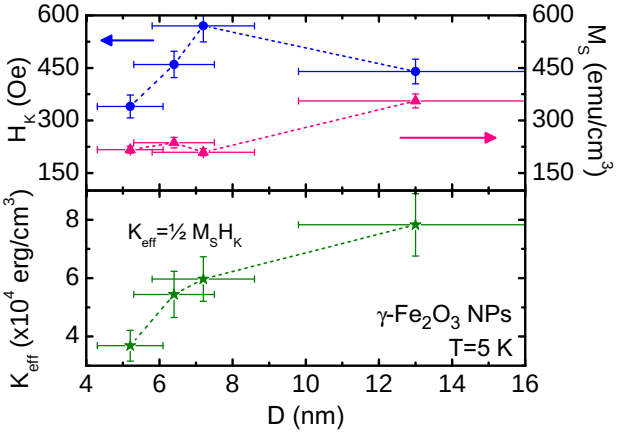

Figure 5: (top panel) H_{K} and M_{S} values as obtained from the TS scans and M(H) measurements, respectively. (bottom panel) K_{eff} estimated from H_{K} and M_{S} values. The three parameters are plotted as a function of the particle diameter.

4 Conclusions

The increasing asymmetry in the peak heights in the TS scans of γ-Fe_2O_3 NPs samples is due to a combination of the anisotropy field distribution given by the size distribution in the samples, and the interparticle interactions that increase as the particle size increases. K_{eff} values determined from the TS measurements for the particles are found to be close to those of bulk maghemite and increase as the particle diameter increases. These values, however, are lower than those previously determined for the same NPs systems in Ref. [8]. Such a difference may be due to the influence of interparticle interactions and anisotropy field distribution in the determination of H_{K} from TS measurements. The effects of interparticle interaction in this maghemite system overcome those of thermal fluctuations, in contrast with the behavior observed in other iron oxide particles such as SiO_2 - coated $Fe_{3-x}O_4$ NPs [12].

Acknowledgments

The financial support of the Spanish MINECO MAT2011-23791, MAT2014-53921-R, and MAT2014-54975-R and Aragonese DGA-IMANA E34 and M4 projects is acknowledged. Au-

thors also acknowledge the Servicio General de Apoyo a la Investigacion-SAI, Universidad de Zaragoza.

References

[1] Amstad, E., Textor, M., and Reimhult, E. *Nanoscale* **3**, 2819–2843 (2011).

[2] Urtizberea, A. *Open problems in the magnetic behavior of iron-oxide nanoparticles.* PhD thesis, Universidad de Zaragoza, (2011).

[3] Ling, D. and Hyeon, T. *Small* **9**(9-10), 1450–1466 (2013).

[4] Özdemir, O. and Banerjee, S. K. *Geophys. Res. Lett.* **11**(3), 161–164 (1984).

[5] Gehring, A. U., Fischer, H., Louvel, M., Kunze, K., and Weidler, P. G. *Geophys. J. Int.* **179**(3), 1361–1371 (2009).

[6] Martínez, B., Obradors, X., Balcells, L., Rouanet, A., and Monty, C. *Phys. Rev. Lett.* **80**, 181–184 Jan (1998).

[7] Millán, A., Urtizberea, A., Silva, N. J. O., Palacio, F., Amaral, V. S., Snoeck, E., and Serin, V. *J. Magn. Magn. Mat.* **312**, L5–L9 (2007).

[8] Komorida, Y., Mito, M., Deguchi, H., Takagi, S., Millán, A., Silva, N. J. O., and Palacio, F. *Appl. Phys. Lett.* **94**, 202503 (2009).

[9] Poddar, P., Morales, M. B., Frey, N. A., Morrison, S. A., Carpenter, E. E., and Srikanth, H. *J. Appl. Phys.* **104**, 063901 (2008).

[10] Frey, N. A. *Surface and interface magnetism in nanostructures and thin films.* PhD thesis, University of South Florida, (2008).

[11] Spinu, L., O'Connor, C. J., and Srikanth, H. *IEEE Trans. Magn.* **37**, 2188 (2001).

[12] Figueroa, A. I., Moya, C., Bartolomé, J., Bartolomé, F., García, L. M., Pérez, N., Labarta, A., and Batlle, X. *Nanotechnology* **25**, 155705 (2013).

[13] Figueroa, A. I., Bartolomé, J., García del Pozo, J. M., Arauzo, A., Guerrero, E., Téllez, P., Bartolomé, F., and García, L. M. *J. Magn. Magn. Mat.* **324**, 2669–2675 (2012).

[14] Aharoni, A., Frei, E. H., Shtrikman, S., and Treves, D. *Bull. Res. Counc. of Israel* **6A**, 215–238 (1957).

[15] Matarranz, R., Contreras, M. C., Pan, G., Presa, B., Corrales, J. A., and Calleja, J. F. *J. Appl. Phys.* **99**, 08Q504 (2006).

[16] Dormann, J. L., D'Orazio, F., Lucari, F., Tronc, E., Prené, P., Jolivet, J. P., Fiorani, D., Cherkaoui, R., and Noguès, M. *Phys. Rev. B* **53**, 14291–14297 Jun (1996).

[17] Yoon, S. *J. Korean Phys. Soc.* **59**(5), 3069–3073 (2011).

[18] Poddar, P., Wilson, J. L., Srikanth, H., Farrell, D. F., and Majetich, S. A. *Phys. Rev. B* **68**, 214409 Dec (2003).

[19] Pfeiffer, H. *Phys. Status Solidi (a)* **118**(1), 295–306 (1990).

[20] de Julián Fernández, C. *Phys. Rev. B* **72**, 054438 Aug (2005).

[21] Pfeiffer, H. *Phys. Status Solidi (a)* **120**(1), 233–245 (1990).

[22] Pfeiffer, H. and Schüppel, W. *Phys. Status Solidi (a)* **119**(1), 259–269 (1990).

[23] Batlle, X., Garcia del Muro, M., Tejada, J., Pfeiffer, H., Gornert, P., and Sinn, E. *Journal of Applied Physics* **74**(5), 3333–3340 (1993).

[24] Valstyn, E. P., Hanton, J. P., and Morrish, A. H. *Phys. Rev.* **128**, 2078 (1962).